Hydrometallurgy 178 (2018) 60–76

Contents lists available at ScienceDirect

Hydrometallurgy

journal homepage: www.elsevier.com/locate/hydromet

Fractional order fuzzy PID optimal control in copper removal process of zinc hydrometallurgy

Fengxue Zhang, Chunhua Yang*, Xiaojun Zhou, Hongqiu Zhu

School of Information Science and Engineering, Central South University, Changsha 410083, PR China

ARTICLE INFO

Keywords:
Copper removal process
Disturbance rejection
Fractional order calculus
Fuzzy logic control
PID control
State transition algorithm

ABSTRACT

The copper removal process is the first stage of purification in zinc hydrometallurgy. Due to its dynamic characteristics and complex reaction mechanism, a robust and effective controller to maintain high quality and stability of the outlet-ion-concentration is in great need. In this paper, a fractional order fuzzy proportional integral derivative (FOFPID) controller based on fuzzy logic is proposed to meet this challenge. The proposed work is conducted through a combination of three novel interdependent efforts. First, controller design problem is transformed into a nonconvex optimization problem. Second, a novel method named state transition algorithm (STA) is employed to solve the aforementioned optimization problem. Furthermore, in order to evaluate the performance of the proposed control strategy, the response performance of the system is analyzed. Finally, further tests are carried out to evaluate the performance of FOFPID controller, where disturbances caused by the measurement, flow rate, and inlet-ion-concentration are all taken into account. The simulation results demonstrate the superiority of the FOFPID controller in copper removal process over the competing FOPID and manual control in the same application environment.

1. Introduction

Zinc hydrometallurgy is the main process in zinc manufacture, as shown in Fig. 1, where it consists of roasting, leaching, purification, electrowinning, and casting (Laatikainen et al., 2010). At present, more than 80% of zinc metal productions globally are produced based on this technique (Balarini et al., 2008). However, in the leaching process, other metallic impurities, such as copper, cobalt, nickel, and cadmium, are also leached (Sun et al., 2014). The existence of these impurity metal ions in zinc solution causes large reductions of current efficiency in electrowinning as well as the quality of the zinc ingot (Xie et al., 2015). Therefore, sufficient purification of zinc solution, which removes the impurities to an acceptable level before electrowinning, is quite essential (Li et al., 2012).

Copper, the major impurity in leaching sulfate solution, must be removed in the first stage of zinc purification (Zhang et al., 2013). In the copper removal process, copper ions are required to be reduced into a desired range to afford enough activators for the next cobalt removal process (by adding metallic zinc) (Zhang et al., 2016b), where the amounts of zinc powder determine the quality and stability of the final products. However, in the actual copper removal process, there are many uncertainties (for example, the competitive relations between two major removal reactions, the fluctuation of inlet-ion-concentrate, the changeable flow rate, and so on) which brings difficulties in the setting of zinc-amounts. Meanwhile, the outlet-copper-concentration is not always kept stable (can't meet the requirement of the next removal process), and the amounts of zinc powder are not efficiently used based on the above considerations. Currently, in order to deal with some disturbances in the system, lots of contributions have been made by researchers (Chen et al., 2017; Sakthivel et al., 2016; Shi et al., 2016). However, copper removal process is a complex nonlinear procedure with long time lag, the above control methods are not suitable to such system. Hence, the main purpose of this paper is to design an optimal control strategy such that the effluent copper impurities in the zinc solution can be reduced to an acceptable level, while consuming the least amount of zinc powder.

Proportional integral derivative (PID)-type controllers are undoubtedly one of the most common control methods used in industries because of their practical utilities (Efe, 2011; Takahashi, 2016; Liu and Wang, 2017). The relative simpler structures make them easily to be implemented, and the refinement and availability of the rules used to tune the parameters of the controllers are the primary reasons for their preference in industrial applications. In classical PID control, there are four weaknesses such as 1) error computation: setpoint is often given as a step function, it amounts to asking the control signal to make a sudden jump; 2) noise degradation in the derivative control: PID is

* Corresponding author.
E-mail address: ychh@csu.edu.cn (C. Yang).

https://doi.org/10.1016/j.hydromet.2018.03.021
Received 26 August 2017; Received in revised form 8 March 2018; Accepted 23 March 2018
Available online 11 April 2018
0304-386X/

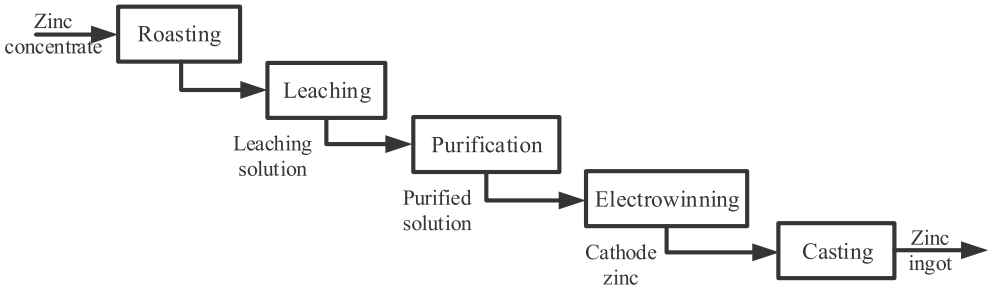

Fig. 1. Flowchart of zinc hydrometallurgy.

often implemented without the D part because of the noise sensitivity; 3) oversimplification: the loss of performance in the control law in the form of a linear weighted sum; 4) complications brought by the integral control: the integral term, while critical to rid of steady-state error, introduces other problems such as saturation and reduced stability margin due to phase lag (Han, 2009). Therefore, classical PID controller fails to provide an effective control to a highly nonlinear and coupled system which possesses uncertain behavior (Sharma et al., 2014).

For the purpose of achieving more favorable dynamic performance and robustness of PID control systems, Podlubny proposes a generalization of the PID controllers, namely, fractional-order PID ($PI^{\lambda}D^{\mu}$) controllers (Podlubny, 1999). Both λ (integral order) and μ (differential order) are fractions, the orders of differential term and integral term expand to fractional domain that can increase the flexibility and robustness of the controller (Cao and Cao, 2006). Hence, there are numerous $PI^{\lambda}D^{\mu}$ controllers proposed to be employed in engineering problems. Koksal et al. (Erenturk, 2013) present the application of a fractional-order $PI^{\lambda}D^{\mu}$ controller to a nonlinear two-mass drive system. In Gao et al. (2013), a typical fractional order PID control strategy is employed for the gun control system. Application of fractional order PID controller to an automatic voltage regulator (AVR) system is explored in Zamani et al. (2009); Ramezanian et al. (2013). Monje et al. (2010) apply the $PI^{\lambda}D^{\mu}$ controller to a low pressure flowing water circuit control system. Lots of other intelligent techniques, such as fuzzy logic, neural network, and neuro-fuzzy, are also applied in this type of controller by scientists and researchers. Among these proposed theories, fuzzy logic has turned out to be the most successful and popular in industries, named as fuzzy logic controller (FLC) (Kumar et al., 2011). Interestingly, there are some contributions on $PI^{\lambda}D^{\mu}$ controllers on the basis of fuzzy logic. Saptarshi et al. (Das et al., 2013) apply the fractional order hybrid fuzzy controllers to some oscillatory fractional order processes, and the performance comparison shows that this controller is capable of obtaining a better control. In Mishra et al. (2015), a fractional order fuzzy PID (FOFPID) controller is used to control the binary distillation column system. In Sharma et al. (2016), two-layered fractional order fuzzy logic controllers are applied to the robotic manipulator with variable payload. Kumar et al. (Kumar and Rana, 2017) present a nonlinear adaptive fractional order fuzzy proportional integral derivative (NLA-FOFPID) controller to control a nonlinear, coupled, multi-input and multi-output and uncertain system i.e. a 2-link planar rigid robotic manipulator with payload. In Sahu et al. (2015), a novel fuzzy proportional-integral-derivative (PID) controller is designed for automatic generation control (AGC) of a two unequal area interconnected thermal system. It is obvious that there are many superiorities and applications of $PI^{\lambda}D^{\mu}$-type controller. Hence, we extend it in the copper removal process to obtain better results.

However, how to determine the key parameters (apart from the usual tuning parameters of the classical PID) remains a main challenge in designing $PI^{\lambda}D^{\mu}$ controller. According to our best knowledge, there is no systematic way to set the fractional order parameters because of the complexity of $PI^{\lambda}D^{\mu}$ controller. Therefore, a novel method for tuning the parameters of $PI^{\lambda}D^{\mu}$ controller is in great demand.

State transition algorithm (STA) is a novel optimization method based on the concept of state and state transition for global optimization (Zhou et al., 2012; Zhou et al., 2018; Han et al., 2017c; Huang et al., 2017). Its strong global search ability and adaptability have been demonstrated in several real-world applications. The continuous state transition algorithm is used to resolve the overlapping linear sweep voltammetric peaks in the case of small signals overlapping to a very big one, which can simultaneously determine trace amounts of Cd^{2+} and Co^{2+} in the presence of a high concentration of Zn^{2+} (Wang et al., 2016). A multi-objective state transition algorithm is proposed for solving the optimization problem arising in iron precipitation of zinc hydrometallurgy (Han et al., 2017a). Furthermore, in Zhang et al. (2016c), STA is introduced to select the optimal continuous $PI^{\lambda}D^{\mu}$ controller parameters. In this paper, we follow this research direction and propose STA to be applied to solve the problems of $PI^{\lambda}D^{\mu}$ controller design and the optimal control of copper removal process.

In what follows, the contributions of this paper are summarized: (i) A novel FOFPID controller is extended to obtain optimal performance in copper removal process, and the implementation of this controller is transformed into a nonconvex optimization problem. (ii) A metaheuristic method named STA is introduced to carry out the aforementioned design problem. (iii) Tests are carried out to evaluate the performance of FOFPID controller, where disturbances caused by the measurement, flow rate, and inlet-ion-concentration are all taken into account.

The remainder of the paper is organized as follows. Section 2 introduces the copper removal process control system, which contains the process description, analysis, and modeling, as well as the objective function. Then the structure of FOPID controller and FOFPID controller are proposed in Section 3, the optimal control strategy is also put forward in this section. In Section 4, some simulation results are presented to illustrate the effectiveness of the proposed approach. The main conclusions of this paper are given in Section 5.

2. Copper removal process control system

Copper removal is the first step of the solution purification process in zinc hydrometallurgy (Fig. 2), this is because copper ions are of the highest content among all impurities and of which the standard potential is the largest, that leads to the preferential reaction between zinc and copper. In this section, a dynamic model of this process control system is considered based on the mechanism analysis.

2.1. Process description and analysis

Copper ions are the primary impurities in zinc hydrometallurgical leaching solution. An excess amount of copper ions could reduce current efficiency during zinc electrowinning, leading to the waste of electricity and downgrade of zinc ingot quality. Nevertheless, a proper quantity of copper is beneficial to the following cobalt removal stage. A deficient quantity of copper ions is incapable of offering sufficient activator in the cobalt removal process, which will reduce the removal

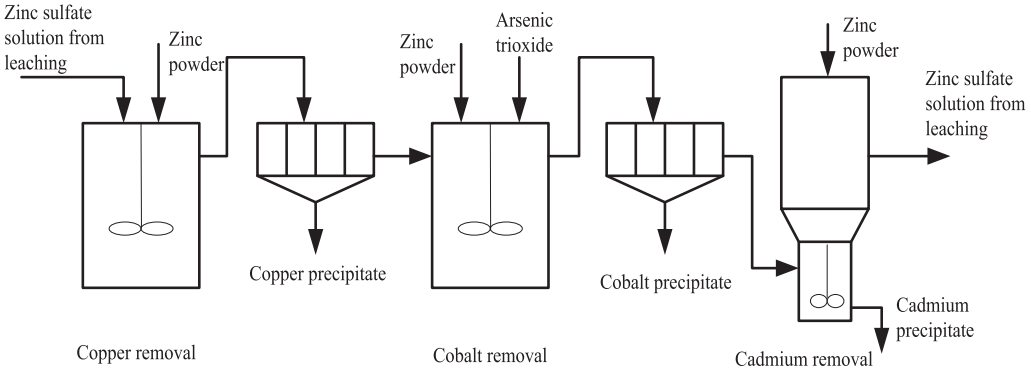

Fig. 2. Solution purification process.

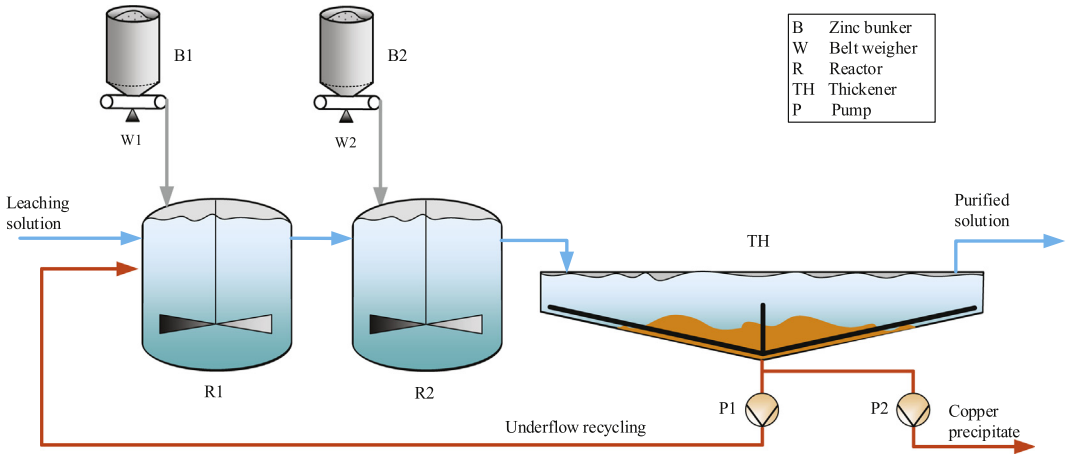

Fig. 3. Flow diagram of copper removal in the zinc purification process.

efficiency of the next cobalt removal stage. Hence, copper ions ought to be reduced to a required concentration range to prevent zinc electrowinning from negative effects.

As a complex process, copper removal includes related units such as impurity precipitation and solid-liquid separation. As it is shown in Fig. 3, the leached zinc sulfate solution flows into two connected continuous stirred reactors (CSTRs), then the copper ions in the solution are removed mainly in the form of metallic copper and cuprous oxide by adding zinc powder in each reactor continuously. After precipitation, the purified solution moves to a thickener to separate the clean solution from the precipitated mud. Then the solution is sent to the next cobalt removal process, and a portion of precipitate which is utilized for seed crystal returned to the first reactor.

During the copper removal process, the quality of outlet-ion-concentration is determined by the amount of zinc powder which is mainly added to the first reactor because majority of the copper ions is deposited in the first reactor. The last reactor is an auxiliary reactor for fine tuning the outlet concentration; thus, the amount of zinc powder added to this reactor is small. Practically, most of the process variables, such as temperatures, oxidation-reduction potential, pH values, zinc ratio, flow rate are measured and controlled in real-time by a distributed control system. However, the impurity concentrations are unavailable online; thus, they are manually sampled and analyzed every 2 h. The added amounts of zinc powder are adjusted manually based on the measured concentration and the changeable flow rate. Nevertheless, operators' experience may not meet the demands of industrial process production. Hence, in order to promote the stability of production and eliminate the impact of unreasonable human experiences, a process control strategy which is composed of modeling, control and optimization should be developed for copper removal.

2.2. Modeling for copper removal process

The aforementioned copper removal process consists of two major chemical reactions which are able to deposit copper ions: copper cementation and cuprous oxide precipitation, as shown in Eqs. (1) and 2, respectively.

$$CuSO_4 + Zn \rightarrow ZnSO_4 + Cu \downarrow \quad (1)$$

$$CuSO_4 + Cu + H_2O \rightarrow Cu_2O \downarrow + H_2SO_4. \quad (2)$$

The ionic copper is firstly reacted with zinc powder and precipitated as metallic copper. And then parts of copper ions react continuously with the precipitated metal and produce cuprous oxide. These two reactions occur simultaneously in the same reactors. The precipitated copper particles in the former reaction are reactants in the latter reaction, while both reactions consume copper ions in the solution. These reactions comprise a typical competitive consecutive reaction system, and the rate of change of the copper ion concentration in the removal reactors was first proposed in Zhang et al. (2016a), which can be simplified as Eq. (3).

$$\begin{cases} r_{Cu^{2+},1} = (\alpha_1 G_{Zn,1} + \alpha_2) V^{-1} C_{Cu^{2+},1} \\ r_{Cu^{2+},2} = (\alpha_3 G_{Zn,2} + \alpha_4) V^{-1} C_{Cu^{2+},2}, \end{cases} \quad (3)$$

where $r_{Cu^{2+},i}$, $i = 1, 2$ is the reaction rate of the copper ion concentration in the ith reactor, α_1, α_2, α_3 and α_4 are the unknown dimensional constants needing to be estimated, $C_{Cu^{2+},i}$, $i = 1, 2$ is the copper ion concentration in the ith reactor, $G_{Zn,i}$, $i = 1,2$ denotes the amounts of zinc powder added in the ith reactor.

The CSTR model of the two reactors can be depicted by the undermentioned differential equations on the basis of the copper removal process flow sheet (Xie et al., 2017)

$$\begin{cases} V\dot{C}_{Cu^{2+},1} = QC^0_{Cu^{2+},1} - (Q+q)C_{Cu^{2+},1} - Vr_{Cu^{2+},1} \\ V\dot{C}_{Cu^{2+},2} = (Q+q)C^0_{Cu^{2+},2} - (Q+q)C_{Cu^{2+},2} - Vr_{Cu^{2+},2}, \end{cases} \tag{4}$$

where $\dot{C}_{Cu^{2+},i}$, $i = 1, 2$ is the rate of change of copper ion concentration in the ith reactor, $C^0_{Cu^{2+},i}$, $i = 1, 2$ is the inlet-copper-concentration of the ith reactor, V is the volume of the reaction solution, Q and q are the flow rates of leached zinc sulfate solution and the returned underflow, respectively.

From the above analysis, the added amount of zinc powder and copper ion concentration can be considered as manipulated variable and state variable, respectively. Let the state variable be $\boldsymbol{x} = [C_{Cu^{2+},1}, C_{Cu^{2+},2}]$, the inlet-copper-concentration be $\boldsymbol{x}_0 = [C^0_{Cu^{2+},1}, C^0_{Cu^{2+},2}]$ and the manipulated variable be $\boldsymbol{u} = [G_{Zn,1}, G_{Zn,2}]$, then the state model of copper removal process can be described as:

$$\dot{\boldsymbol{x}}(t) = A_1\boldsymbol{x}(t) + A_2\boldsymbol{x}_0(t) + \psi[\boldsymbol{x}(t), \boldsymbol{u}(t)] := \boldsymbol{f}(\boldsymbol{x}, \boldsymbol{u}, t), \tag{5}$$

where,

$$A_1 = \begin{bmatrix} -\frac{Q+q}{V} & 0 \\ 0 & -\frac{Q+q}{V} \end{bmatrix},$$

$$A_2 = \begin{bmatrix} \frac{Q}{V} & 0 \\ 0 & \frac{Q+q}{V} \end{bmatrix},$$

$$\psi[\boldsymbol{x}(t), \boldsymbol{u}(t)] = \begin{bmatrix} -(\alpha_1 u_1(t) + \alpha_2)V^{-1}x_1(t) \\ -(\alpha_3 u_2(t) + \alpha_4)V^{-1}x_2(t) \end{bmatrix}.$$

And then we directly use forward-Euler difference scheme to obtain the discrete-time version of Eq. (5), which has the form

$$\boldsymbol{x}(k+1) = (A_1 h + 1)\boldsymbol{x}(k) + A_2 h\boldsymbol{x}_0(k) + h\psi[\boldsymbol{x}(k), \boldsymbol{u}(k)] := \boldsymbol{g}(\boldsymbol{x}, \boldsymbol{u}, k), \tag{6}$$

where h is the step length.

When the inlet-flow-rate, inlet-copper-concentration, temperature, pH and other process parameters of the copper removal process remain stable, there are four parameters that need to be identified. Based on the complexity of the model, an algorithm is applied to select these unknown parameters. The objective of the identification is to minimize the average variance between C_{out} (measured concentration) and C_{model} (the calculated outlet-concentration of copper removal process model):

$$\min F = \frac{1}{N_T}\sum_{j=1}^{N_T}(C_{out}(j) - C_{model}(j))^2, \tag{7}$$

where N_T is the number of test samples.

After modeling the copper removal process, the optimal control problem should be designed. There are two production requirements: (1) keep the outlet-copper-concentration in the desired range, (2) minimize the consumption of zinc powder. Hence, the optimal control objective function for the copper removal process is

$$\min J = \int_0^{t_f}[u_1(t) + u_2(t)]dt$$

$$s.\ t. \begin{cases} \dot{\boldsymbol{x}} = \boldsymbol{f}(\boldsymbol{x}, \boldsymbol{u}, t) \\ \boldsymbol{x}_0 = [C^0_{Cu^{2+},1}, C^0_{Cu^{2+},2}] \\ C_{Cu^{2+},\min} \le x_2(t) \le C_{Cu^{2+},\max} \\ \boldsymbol{u}^{lb} \le \boldsymbol{u}(t) \le \boldsymbol{u}^{ub} \\ t \in [0, t_f], \end{cases} \tag{8}$$

where t_f denotes the final time of the time horizon $[0, t_f]$, $[C_{Cu^{2+},\min}, C_{Cu^{2+},\max}]$ is the required range of outlet-copper-concentration and $[\boldsymbol{u}^{lb}, \boldsymbol{u}^{ub}]$ depicts the bound constraints of the manipulated variables $\boldsymbol{u}(t)$.

The objective function and constraints in Eq. (8) are discretized and the results are given in Eq. (9).

$$\min J = \sum_{k=0}^{M}[u_1(k) + u_2(k)]$$

$$s.\ t. \begin{cases} \boldsymbol{x}(k+1) = \boldsymbol{g}(\boldsymbol{x}(k), \boldsymbol{u}(k), k) \\ \boldsymbol{x}_0 = [C^0_{Cu^{2+},1}, C^0_{Cu^{2+},2}] \\ C_{Cu^{2+},\min} \le x_2(k) \le C_{Cu^{2+},\max} \\ \boldsymbol{u}^{lb} \le \boldsymbol{u}(k) \le \boldsymbol{u}^{ub} \\ k \in [0, M], \end{cases} \tag{9}$$

where M represents the sample size.

The copper removal process system is dynamic and non-linear, and thus their optimal control becomes a challenging task. Conventional controllers, such as proportional-integral-derivative (PID), fail to provide satisfactory performance for such process with nonlinear and uncertain dynamics (Miccio and Cosenza, 2014), thereby application of an expert and intelligent system is desired for effective control of this process. The introduction of fuzzy logic, in the world of control theory, has remarkably enhanced the applicability controllers to control the complex and nonlinear plants due to its several advantages over classical approaches such as involvement of human expertise, model-free and flexible approach (Sharma et al., 2016). In addition, the control engineers always strive for inclusion of additional parameters in the controller as it offers more design freedom. In many recent research works, a more flexible variant of the operator in conventional PID controller, fractional order operator s^κ, where κ is a non-integer, has been used to make control systems more robust and give an additional degree of freedom to the control engineer (Mishra et al., 2015). Hence, we present a hybrid scheme with combination of fractional-order PID and fuzzy logic for the copper removal process system.

3. Structures of FOPID and FOFPID controllers

In this section, structures of FPOID and FOFPID controllers are discussed. The transfer function of $PI^\lambda D^\mu$ controller, which was proposed by Podlubny (Podlubny, 1999) for the first time, has the form

$$G_c(s) = \frac{u(s)}{e(s)} = k_p + k_i s^{-\lambda} + k_d s^\mu. \tag{10}$$

where k_p,k_i and k_d represent the proportional, integral and differential gains, respectively; λ and μ are integral and differential orders correspondingly.

When $\lambda = 1$,$\mu = 1$, there will be a special case of $PI^\lambda D^\mu$ controller:

$$G_c(s) = k_p + \frac{k_i}{s} + k_d s. \tag{11}$$

It is not difficult to find that the above controller is a conventional integer-order PID controller. With the two extra parameters to be adjusted, the fractional-order PID controller is more flexible in controller design.

For industrial application, the form of discrete-time $PI^\lambda D^\mu$ controller needs to be designed. Before we go to the detailed form of such controller, some fundamentals of fractional calculus and the fractional operator are briefly introduced.

3.1. Fractional order calculus

Fractional order calculus, denoted as ${}_{t_0}\mathscr{D}_t^\kappa$, is a generalization of integration and differentiation to the non-integer order operator, which can be expressed as

$$ {}_{t_0}\mathscr{D}_t^{\kappa} = \begin{cases} \dfrac{d^{\kappa}}{dt^{\kappa}} & \kappa > 0, \\ 1 & \kappa = 0, \\ \displaystyle\int_{t_0}^{t} (d\tau)^{-\kappa} & \kappa < 0, \end{cases} \tag{12} $$

where $\kappa \in \mathbb{R}$ represents the order of the operation i.e. μ and $-\lambda$, t_0 and t represent the lower limit and upper limit of the operation, respectively.

There are several definitions to describe fractional calculus, of which Riemann-Liouville and Grunwald-Letnikov definitions are most widely used.

(1) Riemann-Liouville definition (RL)

$$ {}_{t_0}\mathscr{D}_t^{\kappa} f(t) = \frac{1}{\Gamma(n-\kappa)} \frac{d^n}{dt^n} \int_{t_0}^{t} \frac{f(\tau)}{(t-\tau)^{1-(n-\kappa)}} d\tau \quad n-1 < \kappa < n \tag{13} $$

where $\Gamma(\cdot)$ is the renowned Euler's gamma function, defined by

$$ \Gamma(z) = \int_0^{\infty} t^{z-1} e^{-t} dt, \quad \mathbf{R}(z) > 0. \tag{14} $$

(2) Grünwald-Letnikov definition (GL)

$$ {}_{t_0}\mathscr{D}_t^{\kappa} f(t) = \lim_{h \to 0} \frac{1}{h^{\kappa}} \sum_{i=0}^{[(t-t_0)/h]} (-1)^i \binom{\kappa}{i} f(t-ih), \tag{15} $$

where $(-1)^i \binom{\kappa}{i}$ is the binomial coefficient of $(1-z)^{\kappa}$. A numerical computation method for calculating the fractional calculus can be described as follows

$$ {}_{t_0}\mathscr{D}_t^{\kappa} f(t) = \frac{1}{h^{\kappa}} \sum_{i=0}^{[(t-t_0)/h]} w_i^{(\kappa)} f(t-ih), \tag{16} $$

where, h is time step and the definition of $w_i^{(\kappa)}$ are given in Eq. (15),

$$ w_0^{(\kappa)} = 1, \quad w_i^{(\kappa)} = \left(1 - \frac{\kappa+1}{i}\right) w_{i-1}^{(\kappa)}, \quad i = 1, 2, \cdots. \tag{17} $$

The Laplace transformation of fractional derivative and integral of $f(t)$ can be defined by

$$ \begin{aligned} \mathscr{L}\{\mathscr{D}^{-\kappa} f(t)\} &= s^{-\kappa} F(s), \\ \mathscr{L}\{\mathscr{D}^{\kappa} f(t)\} &= s^{\kappa} F(s) - \sum_{i=0}^{n-1} s^l [\mathscr{D}^{\kappa-i-1} f(t)]_{t=0}, \\ & \qquad n-1 < \kappa < n. \end{aligned} \tag{18} $$

The RL definition is equivalent to the GL definition since $\binom{\kappa}{i} = \frac{\Gamma(\kappa+1)}{i!\,\Gamma(\kappa-i+1)}$, while the GL definition is more suitable for numerical calculation, and it is adopted in this study.

3.2. Fractional order operator

In general, the discretization of continuous fractional-order operator s^{κ} ($\kappa \in R$) can be expressed by the generating function denoting the discrete operator, expressed as a function of complex variable z or the shift operator z^{-1}. This generating function and its expansion determine both the forms of the approximation and the coefficients. In this paper, the backward Euler rule is applied which leads to the generating function has the following general form:

$$ s^{\kappa} = \left(\frac{1-z^{-1}}{T}\right)^{\kappa}. \tag{19} $$

However, the fractional-order conversion schemes lead to non-rational z-formulae. Therefore, in order to get rational expressions we expand them into Taylor series and the final algorithm corresponds to a i-term truncated series. In this sense, the generating formula can be tuned more precisely. Moreover, the form of discrete-time fractional-order operator ' D' can be obtained as follows:

$$ D^{\kappa} = \left(\frac{1}{T}\right)^{\kappa} \sum_{i=0}^{\infty} (-1)^i \binom{\kappa}{i} z^{-i}. \tag{20} $$

Hence, the fractional-order operator of a sequence $f(n)$ can be described as Eq. (21) according to Eqs. (15–17) and Eq. (20)

$$ D^{\kappa}(f(n)) = \left(\frac{1}{T}\right)^{\kappa} \sum_{i=0}^{\infty} w_i^{(\kappa)} f(n-i). \tag{21} $$

Clearly, in practice the upper bound of sigmas in Eq. (21) cannot be considered equal to infinity. Restricting the number of the upper bound units to a memory size N, the following formula is proposed:

$$ D^{\kappa}(f(n)) = \left(\frac{1}{T}\right)^{\kappa} \sum_{i=0}^{N} w_i^{(\kappa)} f(n-i). \tag{22} $$

3.3. The form of FOPID controller

In general, Eq. (20) holds for both the positive and negative values of κ. Hence, one may try to expand the integral term of Eq. (10) in a similar manner and arrive at an equation like Eq. (20) in λ, but the problem with such an expansion is that the resulted series doesn't have infinite direct current gain (considering the fact that any infinite series must be truncated in practice), which is essential for tracking the step command without steady-state error (Merrikh Bayat et al., 2014). In order to find a series approximation for $s^{-\lambda}$ in terms of z^{-1} which has infinite direct current gain, first we write it as $s^{-\lambda} = (1/s) \times s^{1-\lambda}$ and then apply Eq. (20) to it. Applying this technique yields

$$ s^{-\lambda} = \left(\frac{1}{T}\right)^{-\lambda} \frac{1}{1-z^{-1}} \sum_{i=0}^{\infty} (-1)^i \binom{1-\lambda}{i} z^{-i}. \tag{23} $$

With combinations of Eqs. (10), (20) and (23) we can obtain the following formulation for the discrete-time $PI^{\lambda}D^{\mu}$ controller

$$ G_c(z) = K_p + K_i \frac{1}{1-z^{-1}} \sum_{i=0}^{N} (-1)^i \binom{1-\lambda}{i} z^{-i} + K_d \sum_{i=0}^{N} (-1)^i \binom{\mu}{i} z^{-i} \tag{24} $$

where

$$ \begin{cases} K_p = k_p, \\ K_i = k_i \left(\dfrac{1}{T}\right)^{-\lambda}, \\ K_d = k_d \left(\dfrac{1}{T}\right)^{\mu}. \end{cases} \tag{25} $$

By using the inverse z-transform and Eq. (22), the difference equation relating $e(k)$ to $u(k)$ can be written as the following:

$$ \begin{aligned} u(k) = {} & u(k-1) + K_p[e(k) - e(k-1)] \\ & + K_i \sum_{i=0}^{N} w_i^{(1-\lambda)} e(k-i) \\ & + K_d \sum_{i=0}^{N} w_i^{(\mu)} [e(k-i) - e(k-i-1)]. \end{aligned} \tag{26} $$

3.4. The form of FOFPID controller

In order to design the structure of FOFPID, the technique of conventional fuzzy PID controller is extended in fractional order domain. And it leads to the combination of fractional order fuzzy PI and fuzzy PD controllers.

3.4.1. Fuzzy PID controller

In the frequency domain, the output of the PI and PD controllers can be written as

$$ s u_{PI}(s) = k_p s e(s) + k_i e(s), \tag{27} $$

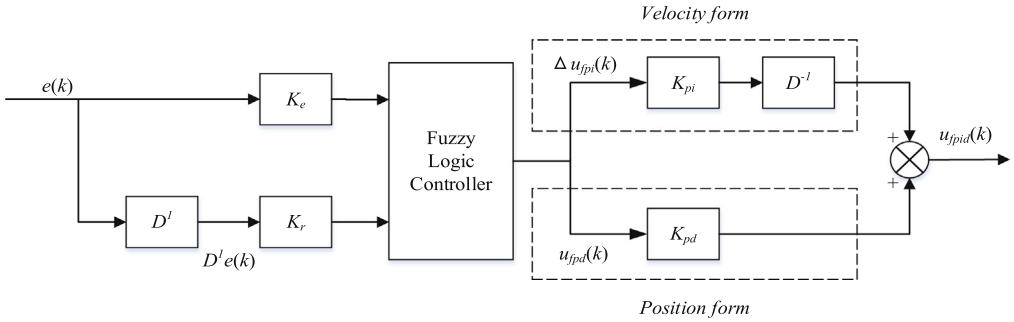

Fig. 4. Structure of FPID controller.

$$u_{PD}(s) = k_p e(s) + k_d s e(s). \tag{28}$$

Then applying backward Euler method and inverse z-transform to discretize the above equation, we can obtain

$$u_{pi}(k) - u_{pi}(k-1) = K_p^{pi}[e(k) - e(k-1)] + K_i^{pi} e(k),$$
$$u_{pd}(k) = K_p^{pd} e(k) + K_d^{pd}[e(k) - e(k-1)]. \tag{29}$$

where K_p^{pi}, K_i^{pi}, K_p^{pd} and K_d^{pd} are the proportional, integral and derivative gains.

Therefore, a simple structure of fuzzy PID controller, which is shown in Fig. 4, is quite often used in present work (Mishra et al., 2015). And the output of the FPID controller is the aggregation of FPI + FPD controllers that can be described as

$$u_{fpid}(k) = \underbrace{K_{pi} D^{-1}[\Delta u_{fpi}(k)]}_{Velocity\ form} + \underbrace{K_{pd} u_{fpd}(k)}_{Position\ form}, \tag{30}$$

where u_{fpid} is the output of FPID controller, D^{-1} is the integer-order integrator, K_{pi} and K_{pd} are the output scaling factors which can offer an additional degree of freedom and enhance the flexibility in FPID controller design.

3.4.2. Fractional order fuzzy PID controller

The structure of FOFPID controller is designed on the basis of the expansion of the FPID controller, as shown in Fig. 5. The only difference between these two sets of fuzzy controllers is that the FOFPID controller uses a fractional order differentiator to produce the rate of change of error as an input of the fuzzy logic controller. Furthermore, it also employs a fractional order integrator to integrate an output of the fuzzy logic controller to form the control action of fuzzy PI. In addition, the implementation of these two controllers uses the same fuzzy logic controller structure but different values of the gains. Hence, the output of the FOFPID controller can be stated as

$$u_{fofpid}(k) = \underbrace{K_{pi} D^{-\lambda}[\Delta u_{fopi}(k)]}_{Velocity\ form} + \underbrace{K_{pd} u_{fopd}(k)}_{Position\ form}. \tag{31}$$

where $D^{-\lambda}$ is the fractional-order integrator.

3.4.3. Implementation of fuzzy logic controller

From Figs. 4 and 5 which were shown in the above two sections, it is necessary to implement the fuzzy logic controllers to design FPID and FOFPID controllers. There are two inputs: error and rate of change of error, required to be fuzzified. Furthermore, the output is the controller output. The process of fuzzy inferencing mainly comprises: a) Fuzzification, b) Rule base, c) Inference engine, d) Defuzzification.

In the copper removal process, the first input of the fuzzy logic controller is the error between the set point and the value of outlet-ion-concentration, which reflects whether the outlet-ion-concentration meets the standard requirement. And second input can represent the future state of the ion concentration. A sharp change rate of the error can cause the ion concentration to return to the desired situation from an undesired situation, whereas it can also cause ion concentration to depart from the desired situation. When the value of ion concentration is equal to the set point without fluctuation, the reaction process must be in a steady state. When the error is equal to zero but has a sharp change rate, the process can not be considered qualified. In contrast, when the ion concentration exceeds the limits but with a good change rate of the error for the concentration to return to the set point, the situation is not as terrible as it seems to be. According to the industrial requirement, the range of the outlet-ion-concentration should be 0.2–0.4 g/L. In this work, we expect the outlet-ion-concentration to stabilize at 0.3 g/L without volatility. And we define that when the outlet-ion-concentration is little low in the range of 0.2 g/L to 0.3 g/L, it is medium-low in the range of 0.1 g/L to 0.2 g/L and very low in the range of less than 0.1 g/L. Conversely, it is a little high in the range of 0.3 g/L to 0.4 g/L, medium-high in the range of 0.4 g/L to 0.5 g/L, and very high in excess of 0.5 g/L. Hence, the error, the change rate of error and the output variables are transformed into seven membership functions namely NL (Negative Large), NM (Negative Medium), NS (Negative Small), ZR (Zero), PS (Positive Small), PM (Positive Medium) and PL (Positive Large) in this work. And since the Gaussian membership function is smooth and nonzero at all points (Ajofoyinbo et al., 2011; Zhao and Bose, 2002), we applied it in both inputs and output. Fig. 6 (a ~ c) shows the membership functions of all variables respectively. In Fig. 6 (a ~ b), ‘ a’ represents the maximal error and the rate of

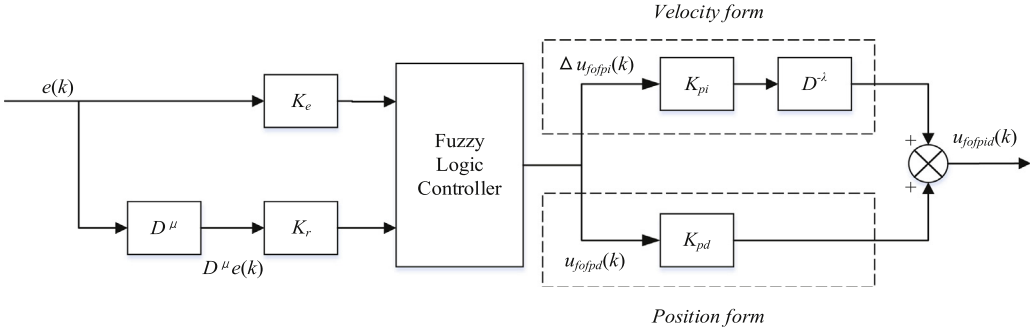

Fig. 5. Structure of FOFPID controller.

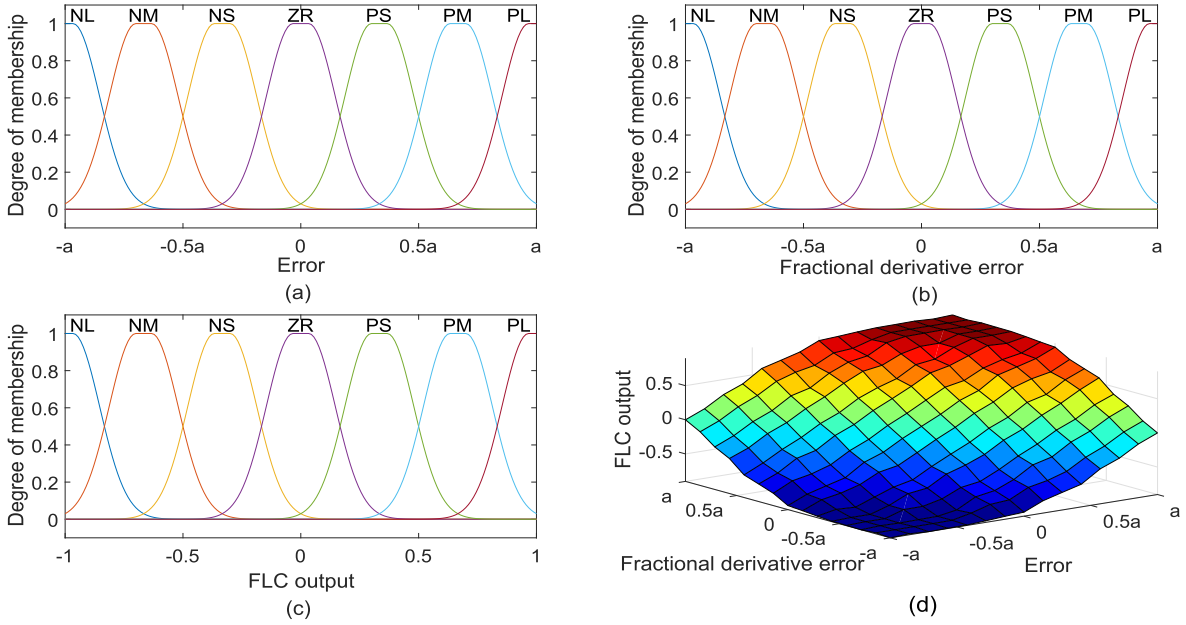

Fig. 6. Fuzzification and defuzzification.

change of error.

Also in this case (Case 01), two-dimensional matrix of the linguistic variables is used, which will result in 49 rules based on the expert's knowledge, process dynamics and experience. The fuzzy rules for the inputs and output are given in Table 1. 'IF-THEN' statements and logical 'AND' operation are used to formulate the rule base.

The inference engine is the central processing unit of a fuzzy logic controller. And on the basis of the contribution of each rule, it can offer suitable control action. In this study, Mamdani min-max inference method (Mamdani and Assilian, 1999) is applied and Fig. 6 (d) shows the surface graph between inputs and output. Then the center of gravity method is applied to defuzzify the fuzzy data.

Then, in order to show how sensitive the results are to the definition of the fuzzy sets, fuzzy sets related to the controller input variables have their parameters slightly modified. That is, the boundary of each fuzzy set was modified. Two different modifications were evaluated, along with the basic situation, forming three studied situations. Based on the basic fuzzy logic controller previously described, the following situations will be investigated: Case 02-the boundaries of input fuzzy sets are reduced by 20%; Case 03-the boundaries of input fuzzy sets are increased by 20%.

The above-mentioned modifications that lead to the fuzzy sets will be applied to the fuzzy logic controller, and the importance of the differences observed in the fuzzy logic controller performance can be evaluated based on the simulation study described in the Section 4.

Remark 1. There is a need to point out that it is a hard work to design the fuzzy controller, especially the fuzzy sets, an expert engineer needs to spend time thinking of the different limits. Hence, this control strategy is not the automatic choice for all processes everywhere, it should be implemented according to the different industrial conditions.

Table 1
Rule base for inputs and output.

		Error						
		NL	NM	NS	ZR	PS	PM	PL
Fractional rate of change of error	NL	NL	NL	NL	NL	NM	NS	ZR
	NM	NL	NL	NL	NM	NS	ZR	PS
	NS	NL	NL	NM	NS	ZR	PS	PM
	ZR	NL	NM	NS	ZR	PS	PM	PL
	PS	NM	NS	ZR	PS	PM	PL	PL
	PM	NS	ZR	PS	PM	PL	PL	PL
	PL	ZR	PS	PM	PL	PL	PL	PL

3.5. Optimization of FOPID and FOFPID controller parameters based on state transition algorithm

The parameter values of the controller determine the performance of the closed loop control. And the optimal control problem of copper removal process can be transformed into finding a set of optimal $PI^{\lambda}D^{\mu}$ parameters to satisfy the requirements of Eq. (9). The block diagram of these two controllers applied to the copper removal process is shown in Fig. 7.

Where $SP\_X_i, i = 1,2$ are the set points of ion concentration, $e_{xi}, i = 1,2$ are errors between the set points and the values of outlet-ion-concentration.

3.5.1. Optimization problem formulation

From the above analysis in Section 2, the optimal control objective is to keep the concentration of outlet copper ions in the desired range and minimizing the consumption of zinc powder. In such cases time integral performance criteria, such as integral squared error (ISE), integral time squared error (ITSE), integral absolute error (IAE) and integral time absolute error (ITAE), will be used. And according to the previous research in Zhang et al. (2016c), ITAE criterion has excellent tracking performance, strong robustness and antidisturbance capability. Therefore, the ITAE criterion and weighting method are used to extend Eq. (8). In the copper removal process, the value of the ion concentration is much smaller than the value of the amount of zinc powder. Hence, the weighting coefficients are added to the objective function to give them the same order of magnitude. The objective function used in this paper can be described as,

$$\min J = \int_0^{t_f} \omega_1(|u_1(t)| + |u_2(t)|) + \omega_2(t|e_{x_1}(t)| + t|e_{x_2}(t)|)dt, \tag{32}$$

and the discrete form is,

$$\min J = \sum_{k=0}^{N} \omega_1(|u_1(k)| + |u_2(k)|) + \omega_2(k|e_{x_1}(k)| + k|e_{x_2}(k)|). \tag{33}$$

where $\omega_i, i = 1,2$ are the weighting coefficients and their values are

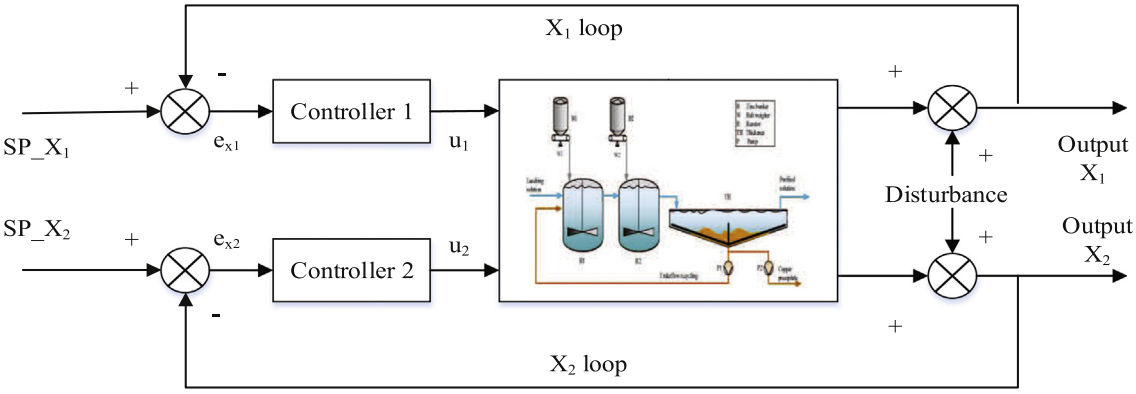

Fig. 7. Block diagram of controllers applied to copper removal process.

determined based on tested industrial data:

$$\begin{cases} \omega_1 + \omega_2 = 1, \\ \omega_1/\omega_2 = \sum_{i=1}^{2}\sum_{j=1}^{L} x_i^j / \sum_{i=1}^{2}\sum_{j=1}^{L} u_i^j, \end{cases} \tag{34}$$

where L is the number of tested industrial data.

Then the optimization algorithm will be used to adjust the controller parameters. Recently, state transition algorithm (STA) has been emerging as a very powerful method for global optimization (Zhou et al., 2012). Hence, we adopt STA to solve the optimal control problem. In the sequel, we will give a brief introduction of state transition algorithm.

3.5.2. A brief description of state transition algorithm

In recent years, a novel stochastic global optimization method named state transition algorithm (STA) has been proposed (Zhou et al., 2016), which is inspired by the notions of state transition and state space representation of control theory. In such a STA method, a solution to an optimization problem can be treated as a state meanwhile the update of current solution using state transformation operators is treated as a state transition. Generally, in continuous state transition algorithm, the unified form of generation of solution can be shown as follows:

$$\begin{cases} \boldsymbol{x}_{k+1} = A_k \boldsymbol{x}_k + B_k \boldsymbol{u}_k \\ y_{k+1} = f(\boldsymbol{x}_{k+1}) \end{cases} \tag{35}$$

where $\boldsymbol{x}_k \in \mathbb{R}^n$ is a state, which corresponds to an optimization problem's solution; A_k and B_k are state transition matrices which has suitable dimensions; $\boldsymbol{u}_k$ is a function of $\boldsymbol{x}_k$ as well as historical states, and f is considered as the evaluation function.

There are four special state transformation operators to generate candidate solutions.

(1) Rotation Transformation (RT)

$$\boldsymbol{x}_{k+1} = \boldsymbol{x}_k + \alpha \frac{1}{n\|\boldsymbol{x}_k\|_2} R_r \boldsymbol{x}_k, \tag{36}$$

where α is defined as the rotation factor and is a positive constant; $R_r \in \mathbb{R}^{n\times n}$ is a random matrix of which elements are within [-1,1]; $\|\cdot\|_2$ is the vector's 2-norm.

(2) Translation Transformation (TT)

$$\boldsymbol{x}_{k+1} = \boldsymbol{x}_k + \beta R_t \frac{\boldsymbol{x}_k - \boldsymbol{x}_{k-1}}{\|\boldsymbol{x}_k - \boldsymbol{x}_{k-1}\|_2}, \tag{37}$$

where β is defined as the translation factor and is a positive constant; $R_t \in \mathbb{R}$ is a random variable of which elements are within [0,1].

(3) Expansion Transformation (ET)

$$\boldsymbol{x}_{k+1} = \boldsymbol{x}_k + \gamma R_e \boldsymbol{x}_k, \tag{38}$$

where γ is defined as the expansion factor and is a positive constant; $R_e \in \mathbb{R}^{n\times n}$ is a random diagonal matrix of which elements obey the Gaussian distribution with mean value 0 and standard deviation 1.

(4) Axesion Transformation (AT)

$$\boldsymbol{x}_{k+1} = \boldsymbol{x}_k + \delta R_a \boldsymbol{x}_k, \tag{39}$$

where δ is defined as the axesion factor and is a positive constant; $R_a \in \mathbb{R}^{n\times n}$ is a random diagonal matrix of which elements obey the Gaussian distribution with mean value 0 and standard deviation 1, and meanwhile there is only one random position having nonzero value.

The procedure of the basic STA can be outlined in the following flowchart, as shown in Fig. 8. Where *SE* is search enforcement which represents the times of transformation by a certain operator, and a new best solution is adopted by using the "greedy criterion". Besides, there are four other important parameters namely rotation factor α, translation factor β, expansion factor γ and axesion factor δ. And *funfcn*, *Best*, *State* represent the objective function, the current best solution and the candidate solution set, respectively. And the specified termination criterion is the maximum number of iterations (Maxiter for short) in this study. In addition, in the case when a better solution can be found by other transformation operators except translation, the translation operator needs to be implemented.

In the continuous state transition algorithm, the rotation transformation can search in a hypersphere when a radius α is given coming from its ability of having the function of local search. The reduction of rotation factor α between a maximum value α_{max} and a minimum value α_{min} obeys an exponential way, of which the base *fc* is defined as lessening coefficient. The translation transformation is designed for a line search. The expansion transformation is developed as a global search operator, which can search in the whole space. The axesion transformation is proposed in the late stage to strengthen the single dimensional search as well as global search.

4. Simulation and results

This section presents the results of simulations under the proposed control strategy, some industrial data in year 2016 is collected from the copper removal process in a zinc hydrometallurgy plant of China. The flow rate is measured on-line and the ion concentration is obtained from manual record every 2 h. The simulation studies are performed within the Matlab environment on a computer.

4.1. Model parameters identification

Identification of the parameters was based on Eq. (7) and the ranges

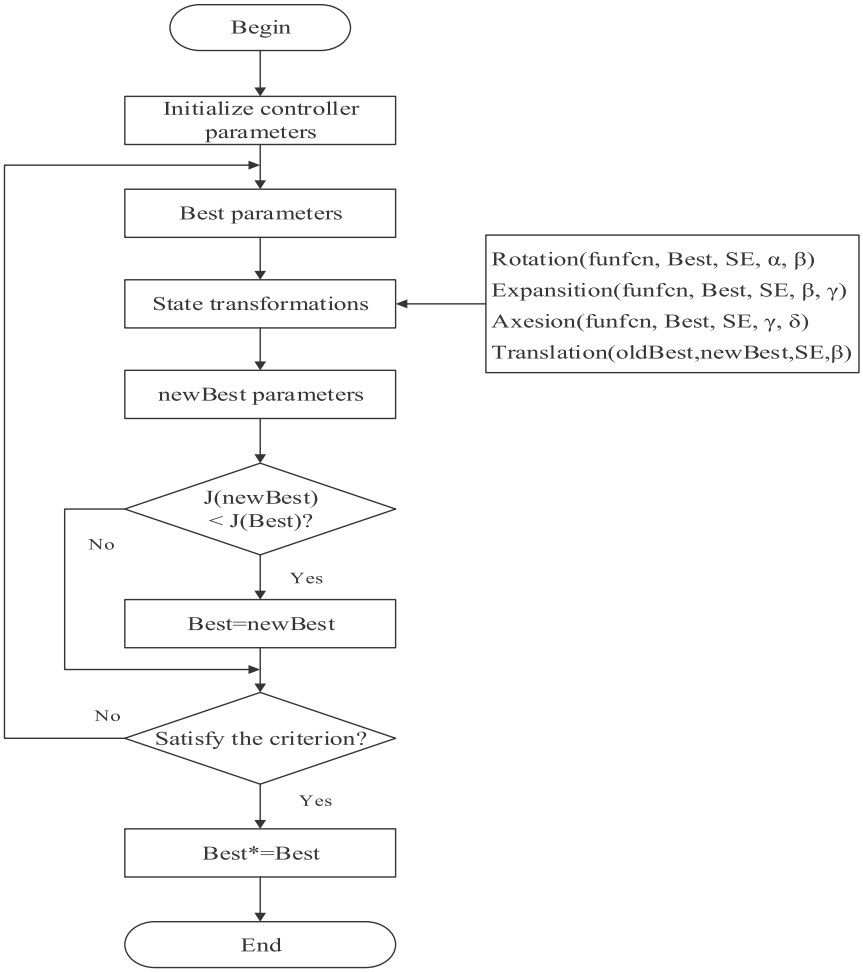

Fig. 8. The flowchart of state transition algorithm.

Table 2
The ranges of input parameters.

ICC (g/L)	IFR (m^3/h)	UR (m^3/h)	ZP (kg/h)	pH	T (C)
0.8-1.8	140-280	6-18	300-720	3.9-4.2	62-66

of data are shown in Table 2.

where ICC, IFR, UR, ZP, pH, and T represent inlet-ion-concentration, inlet-flow-rate, underflow-rate, the amount of zinc powder, pH value, and temperature, respectively.

Then the 84 groups of industrial data which were collected within a week are used for model parameter identification. The flow rate of the solution and the underflow are shown in Fig. 9 (a). The inlet-ion-concentration and outlet-ion-concentration are described in Fig. 9 (b). In addition, STA was run 20 times and 100 iterations for each run. The parameters settings of STA are shown as follow: α is reducing periodically from 1 to 1e-4 in an exponential way, β, γ and δ are all set to 1, all of these are based on the previous paper (Han et al., 2017b). The best results and their 95% confidence interval are given in Table 3. Furthermore, the other 48 groups of industrial data collected over four days are used to validate the copper removal process model. Fig. 10 (a) shows flow rate of the solution and the underflow, Fig. 10 (b) indicates the inlet-ion-concentration, the predicted outlet-ion-concentration and the measured outlet-ion-concentration. Meanwhile, the predicted ion concentration(y-axis) versus actual ion concentration(x-axis), along with a diagonal line indicating equivalence, root mean squared error and R squared value, are shown in Fig. 11. In addition, the min, mean and max errors between the predicted values and the actual values, as well as the relative errors are shown in Table 4.

4.2. Comparative study of FOPID and FOFPID

The design of the controller parameters plays a significant role in the response performance of the closed-loop control system. And the detailed implementation steps of the two fractional order controllers are described in Section 3. The inlet-ion-concentration and the setpoint of X_1 loop are 1.39 and 0.67, respectively. Meanwhile, these two values of X_2 loop are 0.67 and 0.3, respectively. Then PID, FOPID and FOFPID controllers are applied to the simulation of the process so that the outlet-ion-concentration meets the process requirements and the consumption of zinc powder is minimal. Figs. 12 and 13 show the response of the closed-loop systems under three controllers. It is obvious that all the controllers can make the system reach to the setpoint, but the FOFPID controller one can achieve a better response performance (smaller overshoot, shorter rise time and settling time). This means that compared with PID and FOPID controller, FOFPID controller can make the outlet-ion-concentration reach a steady state faster. Also, the values of optimal controller parameters are listed in Tables 5, 6 and 7. In addition, the detailed amount of zinc powder within 2 h under four different control strategies are shown in Fig. 14. In the industrial process, the operator always adds excess zinc powder to ensure the quality of productions, resulting in a lot of waste. From the figure it can be seen that the control strategies proposed in this paper, especially the FOFPID control strategy, make a significant contribution on the reduction of

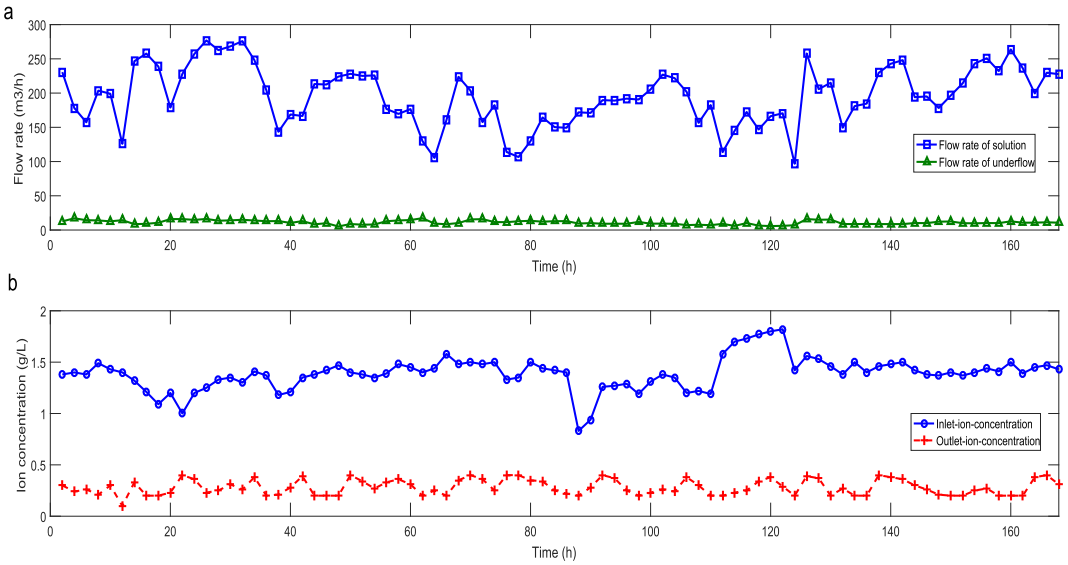

Fig. 9. Flow rate and the ion concentration of the training data.

Table 3
Identification results of model parameters.

Parameter	α_1	α_2	α_3	α_4
Estimation	0.0208	0.1387	0.0003	0.9410
Confidence interval	± 0.0031	± 0.0520	± 2.1e-4	± 0.0270

zinc powder.

Furthermore, simulations for each of the cases considered in the last section were performed to study how sensitive are the results to the definition of the fuzzy sets. The simulation results for the relative steady-state errors are presented in Table 8. Based on the results, it is possible to verify that the modifications made to the fuzzy sets impacted significantly upon performance. The study conducted showed that the definitions of the fuzzy sets of a given fuzzy controller must be taken very carefully as the results are sensitive to small variations in the fuzzy sets. Hence, special care must be taken in defining the fuzzy sets.

4.3. Disturbance rejection

In the industrial process, the measurement noise of the sensor for the outlet-ion-concentration will affect the response performance of the system. In addition, the inlet-flow-rate of impure solution and inlet-ion-concentration will fluctuate in a small range, causing some disturbances to the stability of the system. Therefore, when comparing the performance of these two controllers, the effects of the above disturbances should be taken into account.

4.3.1. Disturbance caused by measurement

The measurement noise of the sensor can be a good test to the performance of controller. An excellent controller should be able to suppress the noise added to the closed loop. To detect the performance of these three controllers to suppress noise, the outlet ion concentration of each reactor are perturbed by ± 5% Gaussian random noise and 20 independent experiments with different random seeds of the Gaussian disturbance model are carried out. Then, we conducted the one-tailed t-test on the relative steady-state errors obtained from the twenty experiments to verify if there is a significant difference among the

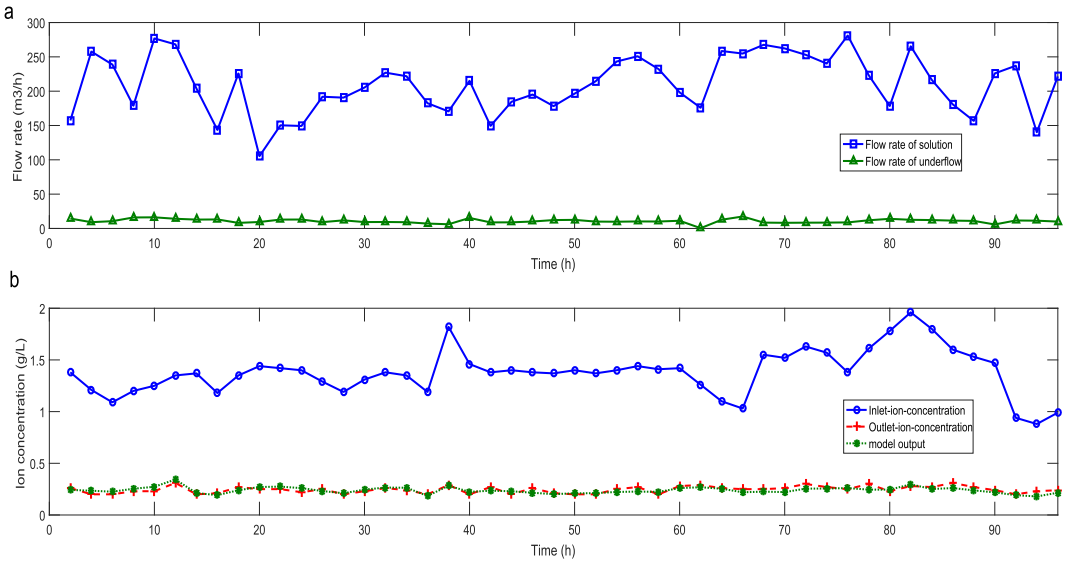

Fig. 10. Flow rate and the ion concentration of the testing data.

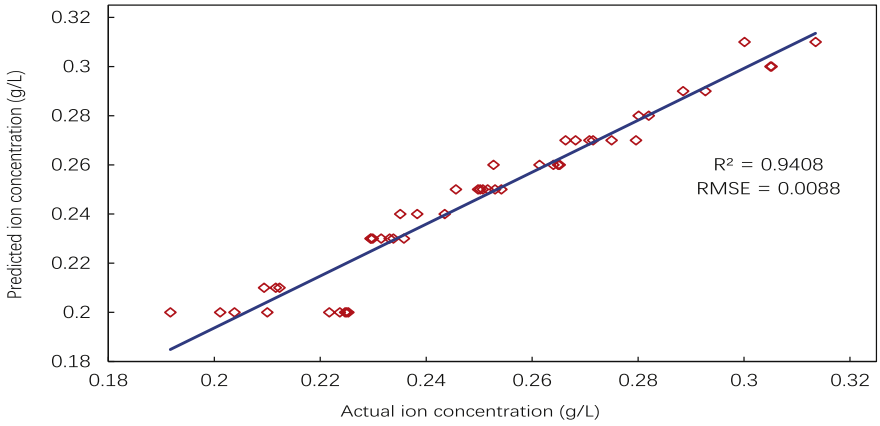

Fig. 11. Predicted ion concentration versus actual ion concentration.

Table 4
Error between model output and measured data.

Max error	Mean error	Min error	Max relative error(%)	Mean relative error(%)	Min relative error(%)
2.53e-3	7.50-4	2.00e-4	9.65e-1	2.45e-1	3.57e-2

controllers. Table 9 shows the results of the one-tailed t-test at a 0.05 significance level. From the one-tailed t-test results, it is obvious that the FOFPID control is superior to PID control in all loops. As for FOPID, the result of X_2 loop indicates that FOFPID control has better performance, and in the X_1 loop they have same performance. In addition, one of the representative response comparison, presented in Figs. 15 and 16, supports that FOFPID controller can offer more robust performance than PID and FOPID controllers in this respect. Furthermore, the total amount of the zinc dust to be added to the two reactors is shown in Fig. 17. From Fig. 17 we can see that the additive amount of zinc dust under the FOFPID controller is the lowest.

4.3.2. *Disturbance through flow rate*

The disturbance caused by the changeable flow rate is a major source of oscillation for the outlet-ion-concentration. And in this paper, a Gaussian noise with standard deviation of ± 5% is introduced in the flow rate. Then, 20 independent experiments are carried out under different random seeds of the Gaussian disturbance model. Figs. 18, 19 and 20 show the corresponding results of one experiment. It is obvious that both the zinc dust consumption and the stability of the process under the FOFPID control are superior to those under the PID control and FOPID control. Again, the results of one-tailed t-test are listed in Table 10.

4.3.3. *Disturbance in inlet ion concentration*

In practice, the zinc solution to be purified is from the previous process. Hence, the inlet-ion-concentration often has fluctuation. In order to simulate the disturbance of inlet-ion-concentration, Gaussian noises with standard deviation of ± 3% is applied. Similarly, we still carry out 20 independent experiments with different random seeds of the Gaussian disturbance model. One of the simulation results are presented in Figs. 21, 22 and 23. And the results for this study revealed that a better optimized control can be obtained through FOFPID controller than PID and FOPID controllers when dealing with variations in inlet-ion-concentration. Table 11 lists the results of one-tailed t-test.

5. Conclusions

In this paper the FOFPID controller based on fuzzy logic is implemented for the copper removal process to deal with the complex dynamic nature of system. The design of FOFPID controller is a parameter optimization problem and there is no systematic way for setting the parameters. Therefore, a control strategy for tuning the parameters based on state transition algorithm is proposed. Besides, a comparative study of the FOFPID controller with conventional FOPID controller and the manual control is carried out to evaluate the performance of the presented control strategies. In addition, to further witness the robustness and effectiveness of the proposed controller, noise suppression is investigated. All the simulation results support that FOFPID

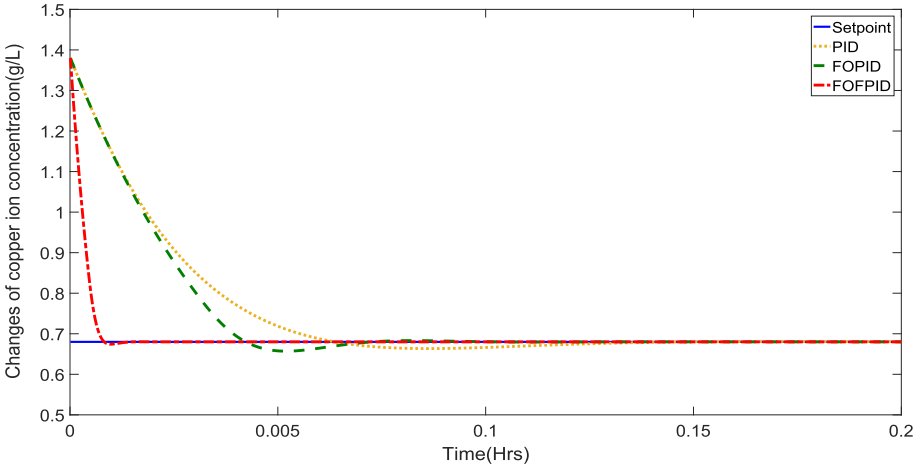

Fig. 12. The changes of outlet-ion-concentration in the first reactor.

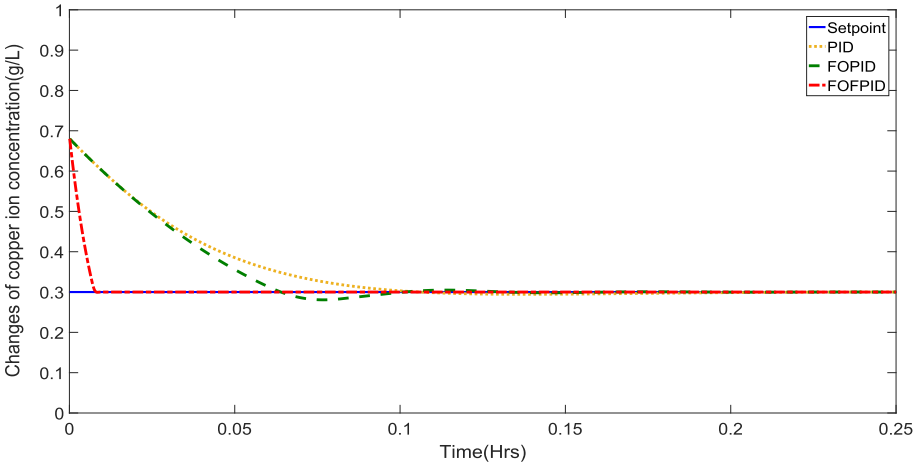

Fig. 13. The changes of outlet-ion-concentration in the second reactor.

Table 5
Optimal tuning results for PID controller.

Process	K_p	K_i	K_d
X_1 loop	49.8650	1.4031	0.0427
X_2 loop	167.0013	7.4281	2.5890

Table 6
Optimal tuning results for FOPID controller.

Process	K_p	K_i	K_d	λ	μ
X_1 loop	0.9492	0.0161	1.8519	6.5836	0.0132
X_2 loop	1.3683	62.4763	0.1945	0.5152	0.0528

Table 7
Optimal tuning results for FOFPID controller.

Process	K_e	K_r	K_{pi}	K_{pd}	λ	μ
X_1 loop	0.8315	0.0336	0.0229	21.8321	0.4508	0.0100
X_2 loop	0.0726	0.0110	238.1530	291.1057	2.4872	4.0861

controller can offer much better performance in disturbance rejection, trajectory tracking and reducing the consumption of materials than other control strategy. Therefore, the proposed controller scheme can be used in the copper removal process industries to handle the problems of suppressing the fluctuation of the outlet-ion-concentration and saving the amount of zinc powder.

Table 8
Simulation results related to the relative steady-state errors in the cases studied.

Process	Case 01	Case 02	Case 03
X_1 loop	2.4157e-03	1.0625e-02	4.0601e-02
X_2 loop	4.0614e-03	1.2744e-02	6.1537e-02

Notations

Equipment

B	Zinc bunker
W	Belt weigher
R	Reactor
TH	Thickener
P	Pump

Variable

$r_{Cu^{2+},i}$	the reaction rate of the ion concentration in the ith reactor ($gL^{-1}h^{-1}$)
$C_{Cu^{2+},i}$	the copper ion concentration in the ith reactor (gL^{-1})
$G_{Zn,i}$	the amounts of zinc powder added in the ith reactor (kg)
$\dot{C}_{Cu^{2+},i}$	the rate of change of ion concentration in the ith reactor ($gL^{-1}h^{-1}$)

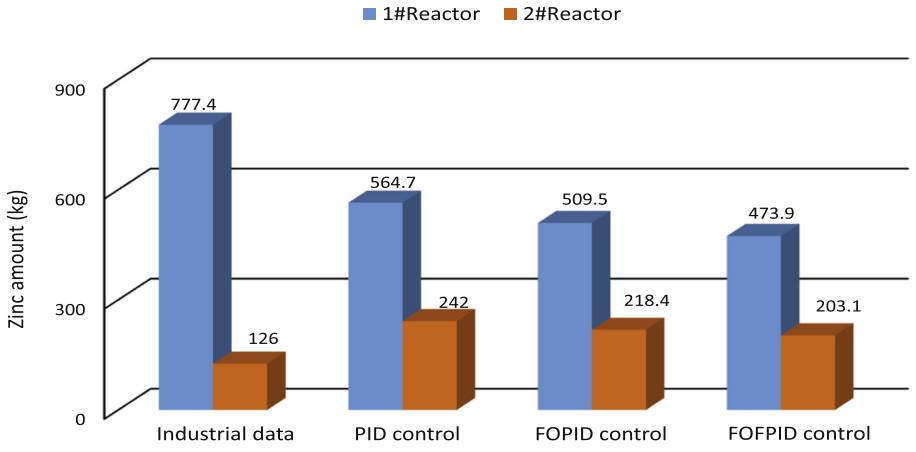

Fig. 14. The consumption of zinc powder under different control strategies.

Table 9
One-tailed t-test at a 0.05 significance level.

Process	PID	FOPID	FOFPID
X_1 loop	6.8759e-02 ± 4.2355e-03 −	2.0430e-02 ± 4.0394e-03 ≈	2.0322e-02 ± 2.9627e-04
X_2 loop	9.8367e-02 ± 6.0547e-03 −	3.4907e-02 ± 5.8926e-03 −	6.5448e-03 ± 1.0079e-04

"−","+",and "≈" denote that the relative steady-state error of the corresponding controller is worse than, better than, and similar to that of FOFPID controller, respectively.

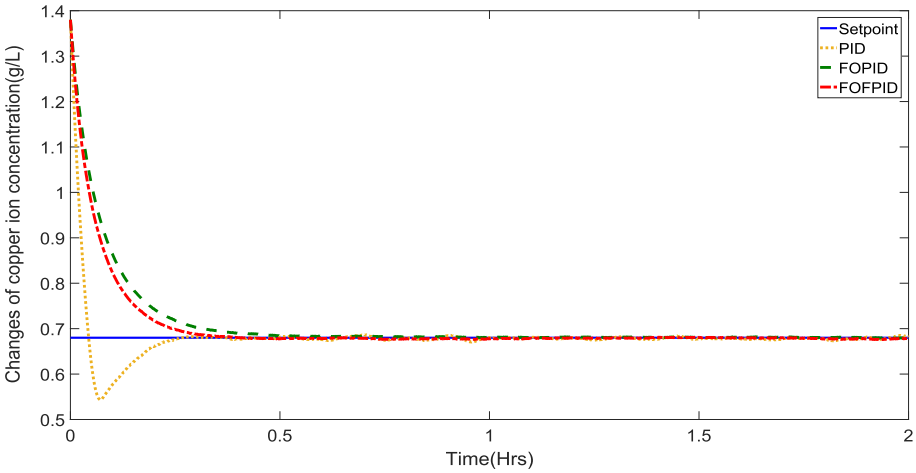

Fig. 15. Outlet-ion-concentration in the first reactor with disturbance of measurement.

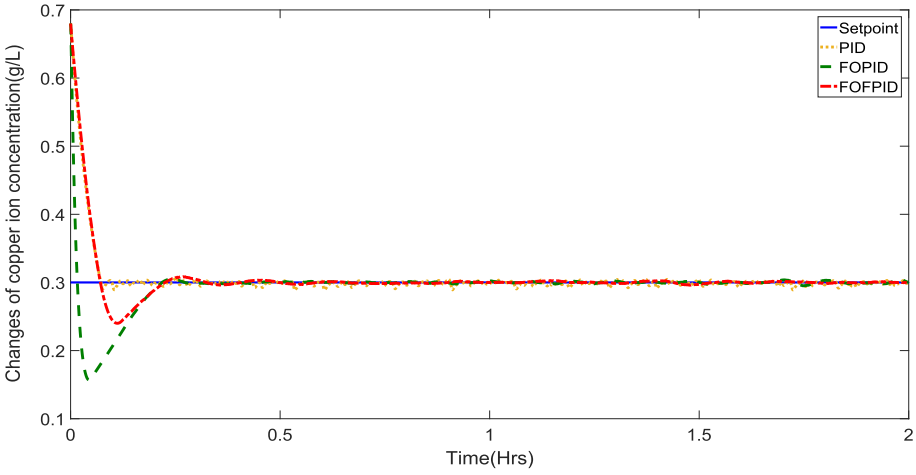

Fig. 16. Outlet-ion-concentration in the second reactor with disturbance of measurement.

$C^0_{Cu^{2+},i}$	the inlet-copper-concentration of the ith reactor (gL^{-1})
V	the volume of the reaction solution (m^3)
Q	the flow rates of leached zinc sulfate solution (m^3h^{-1})
q	the returned underflow (m^3h^{-1})
C_{out}	the measured concentration (gL^{-1})
C_{model}	the calculated outlet-concentration of the model (gL^{-1})
t_f	the final time of the time horizon (h)
α_i	the unknown dimensional constants needing to be estimated
h	the step length
N_T	the number of test samples
M	the sample size
s^κ	the fractional order operator
κ	the non integer order of the operation
${}_{t_0}\mathscr{D}_t^\kappa$	the generalization of calculus to the non-integer order operator
z	the complex variable
N	the memory size
T	the sampling time
k_p	the proportional gain of PID controller
k_i	the integral gain of PID controller
k_d	the differential gain of PID controller
K_p	the proportional gain of FOPID controller
K_i	the integral gain of FOPID controller
K_d	the differential gain of FOPID controller
λ	the integral order FOPID controller
μ	the differential order FOPID controller
K_p^{pi}, K_p^{pd}	the proportional gains of FOFPID controller
K_i^{pi}	the integral gain of FOFPID controller
K_d^{pd}	the differential gain of FOFPID controller
K_{pi}, K_{pd}	the output scaling factor of FOFPID controller
D^{-1}	the integer-order integrator
$D^{-\lambda}$	the fractional-order integrator
K_p^{pi}, K_p^{pd}	the proportional gains of FOFPID controller
K_i^{pi}	the integral gain of FOFPID controller

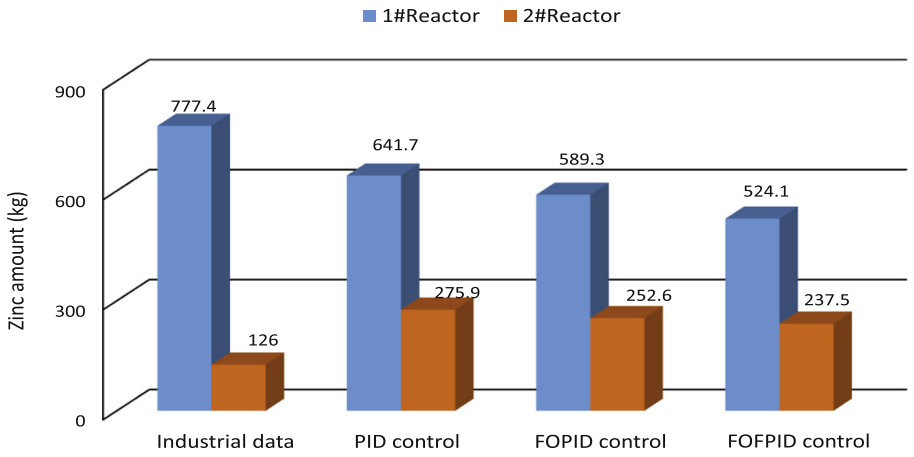

Fig. 17. The consumption of zinc powder with disturbance of measurement.

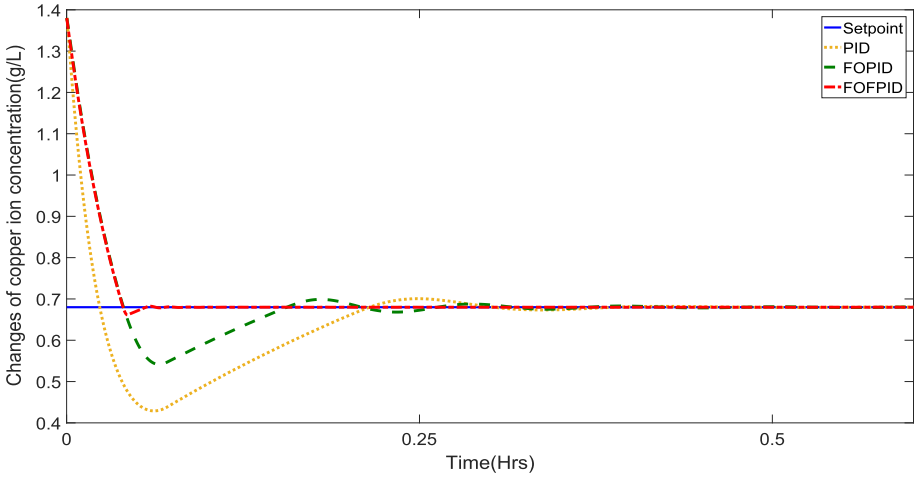

Fig. 18. Outlet-ion-concentration in the first reactor with disturbance of flow rate.

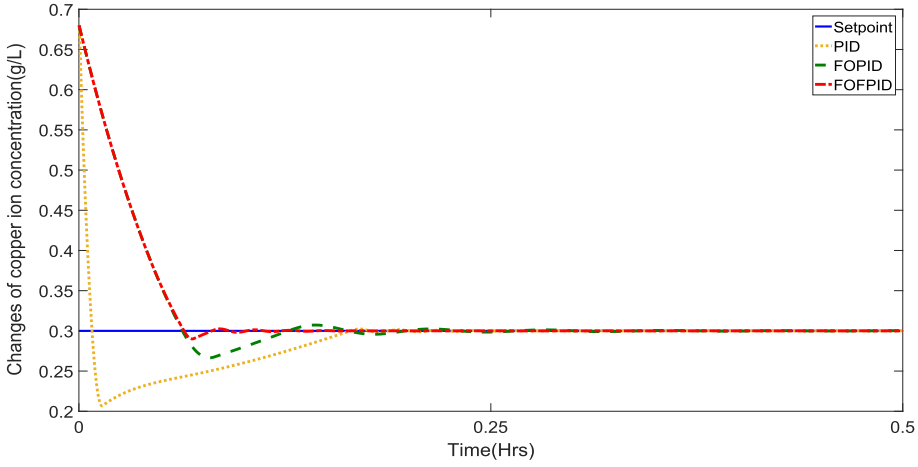

Fig. 19. Outlet-ion-concentration in the second reactor with disturbance of flow rate.

K_d^{pd}	the differential gain of FOFPID controller
ω_i	the weighting coefficients
L	the number of tested industrial data
e_{xi}	the errors between the set points and the values of output
α	the rotation factor in the state transition algorithm
β	the translation factor in the state transition algorithm
γ	the expansion factor in the state transition algorithm
δ	the axesion factor in the state transition algorithm

Compliance with ethical standards

Conflict of Interest

The authors declare that they have no conflict of interest.

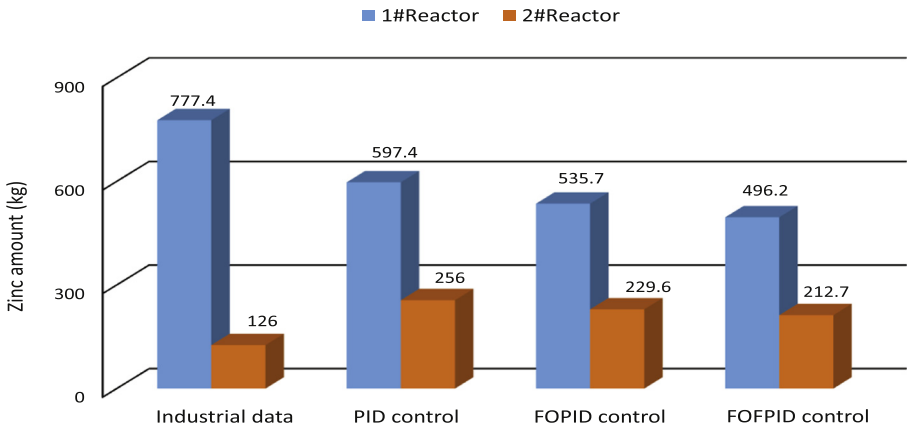

Fig. 20. The consumption of zinc powder with disturbance of flow rate.

Table 10
One-tailed t-test at a 0.05 significance level.

Process	PID	FOPID	FOFPID
X_1 loop	7.7827e-02 ± 6.0857e-03 −	1.1552e-02 ± 5.4868e-03 −	3.5297e-03 ± 1.3543e-04
X_2 loop	8.3567e-02 ± 6.4124e-03 −	1.9029e-02 ± 5.8928e-03 −	5.8903e-03 ± 2.0013e-04

"−","+",and "≈" denote that the relative steady-state error of the corresponding controller is worse than, better than, and similar to that of FOFPID controller, respectively.

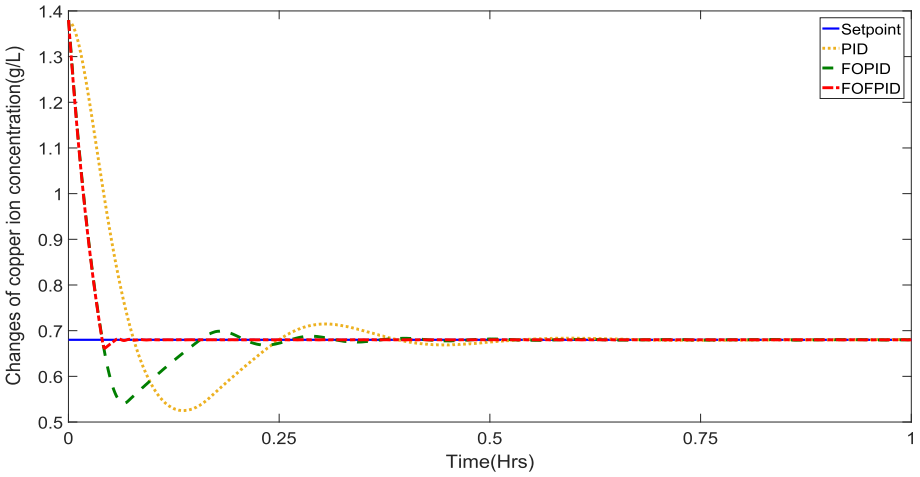

Fig. 21. Outlet ion concentration in the first reactor with disturbance of inlet-ion-concentration.

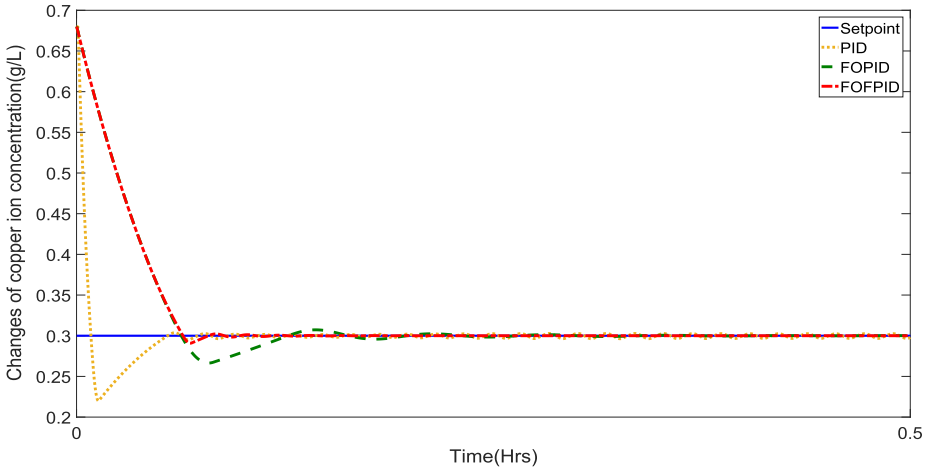

Fig. 22. Outlet ion concentration in the second reactor with disturbance of inlet-ion-concentration.

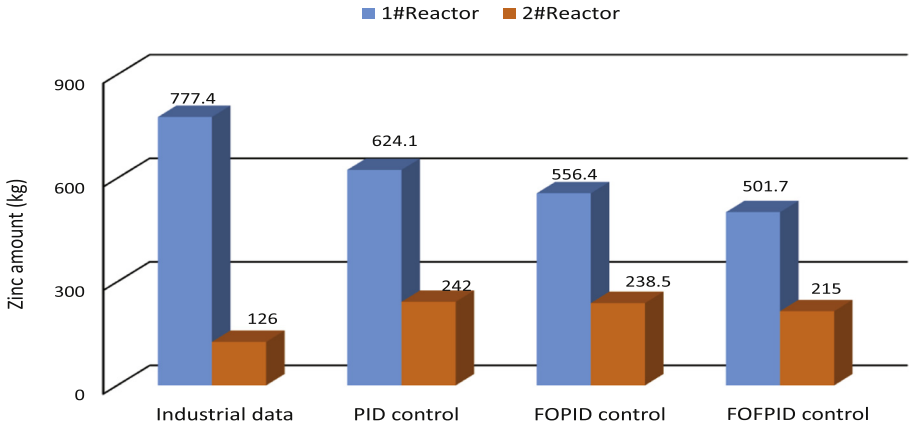

Fig. 23. The consumption of zinc powder with disturbance of inlet-ion-concentration.

Table 11
One-tailed t-test at a 0.05 significance level.

Process	PID	FOPID	FOFPID
X_1 loop	7.9245e-02 ± 5.9469e-03 −	1.1369e-02 ± 5.4817e-03 −	4.3584e-03 ± 1.4586e-04
X_2 loop	7.5813e-02 ± 1.0430e-03 −	2.8957e-02 ± 1.0051e-03 −	1.0187e-03 ± 1.0013e-04

"−","+",and "≈" denote that the relative steady-state error of the corresponding controller is worse than, better than, and similar to that of FOFPID controller, respectively.

Acknowledgments

The work was supported by the National Natural Science Foundation of China (Grant No. 61503416, 61533021, and 61533021), the Foundation for Innovative Research Groups of the National Natural Science Foundation of China (Grant No. 61621062).

References

Ajofoyinbo, A.M., Olunloyo, V.O., Ibidapo-Obe, O., et al., 2011. On development of fuzzy controller: The case of gaussian and triangular membership functions. J. Signal Inform. Process. 2 (4), 257–265.
Balarini, J.C., de Oliveira Polli, L., Miranda, T.L.S., de Castro, R.M.Z., Salum, A., 2008. Importance of roasted sulphide concentrates characterization in the hydro-metallurgical extraction of zinc. Miner. Eng. 21 (1), 100–110.
Cao, J.-Y., Cao, B.-G., 2006. Design of fractional order controllers based on particle swarm optimization. In: 2006 1ST IEEE Conference on Industrial Electronics and Applications, pp. 1–6.
Chen, M., Shao, S.-Y., Shi, P., Shi, Y., 2017. Disturbance-observer-based robust synchronization control for a class of fractional-order chaotic systems. IEEE Trans. Circuits Syst. Express Briefs 64 (4), 417–421.
Das, S., Pan, I., Das, S., 2013. Performance comparison of optimal fractional order hybrid fuzzy pid controllers for handling oscillatory fractional order processes with dead time. ISA Trans. 52 (4), 550–566.
Efe, M.Ö., 2011. Neural Network Assisted Computationally Simple $PI^{\lambda}D^{\mu}$ Control of a Quadrotor UAV. IEEE Trans. Ind. Inf. 7 (2), 354–361.
Erenturk, K., 2013. Fractional-order and active disturbance rejection control of nonlinear two-mass drive system. IEEE Trans. Ind. Electron. 60 (9), 3806–3813.
Gao, Q., Chen, J., Wang, L., Xu, S., Hou, Y., 2013. Multiobjective optimization design of a fractional order PID controller for a gun control system. Sci. World J. 2013 (1) 907256–907256.
Han, J., 2009. From pid to active disturbance rejection control. IEEE Trans. Ind. Electron. 56 (3), 900–906.
Han, J., Yang, C., Zhou, X., Gui, W., 2017a. Dynamic multi-objective optimization arising in iron precipitation of zinc hydrometallurgy. Hydrometallurgy 173, 134–148.
Han, J., Yang, C., Zhou, X., Gui, W., 2017b. A new multi-threshold image segmentation approach using state transition algorithm. Appl. Math. Model. 44, 588–601.
Han, J., Yang, C., Zhou, X., Gui, W., 2017c. A two-stage state transition algorithm for constrained engineering optimization problems. Int. J. Control. Autom. Syst. 1–13. http://dx.doi.org/10.1007/s12555-016-0338-6.
Huang, M., Zhou, X., Huang, T., Yang, C., Gui, W., 2017. Dynamic optimization based on state transition algorithm for copper removal process. Neural Comput. & Applic. 1–13. http://dx.doi.org/10.1007/s00521-017-3232-0.
Kumar, V., Nakra, B., Mittal, A., 2011. A review on classical and fuzzy pid controllers. Int. J. Intell. Control. Syst. 16 (3), 170–181.
Kumar, V., Rana, K., 2017. Nonlinear adaptive fractional order fuzzy pid control of a 2-link planar rigid manipulator with payload. J. Frankl. Inst. 354 (2), 993–1022.
Laatikainen, K., Lahtinen, M., Laatikainen, M., Paatero, E., 2010. Copper removal by chelating adsorption in solution purification of hydrometallurgical zinc production. Hydrometallurgy 104 (1), 14–19.
Li, Y.G., Gui, W.H., Teo, K.L., Zhu, H.Q., Chai, Q.Q., 2012. Optimal control for zinc solution purification based on interacting cstr models. J. Process Control 22 (10), 1878–1889.
Liu, F., Wang, H., 2017. Fuzzy pid tracking controller for two-axis airborne optoelectronic stabilized platform. Int. J. Innov. Comput. Inf. Control. 13 (4), 1307–1322.
Mamdani, E., Assilian, S., 1999. An experiment in linguistic synthesis with a fuzzy logic controller. Int. J. Hum. Comput. Stud. 51 (2), 135–147.
Merrikh Bayat, F., Mirebrahimi, S.N., Khalili, M.R., 2014. Discrete-time fractional-order PID controller: Definition, tuning, digital realization and some applications. Int. J. Control. Autom. Syst. 13 (1), 81–90.
Miccio, M., Cosenza, B., 2014. Control of a distillation column by type-2 and type-1 fuzzy logic pid controllers. J. Process Control 24 (5), 475–484.
Mishra, P., Kumar, V., Rana, K., 2015. A fractional order fuzzy PID controller for binary distillation column control. Expert. Syst. Appl. 42 (22), 8533–8549.
Monje, C.A., Chen, Y., Vinagre, B.M., Xue, D., Feliu-Batlle, V., 2010. Fractional-order systems and controls: fundamentals and applications. Springer Science & Business Media.
Podlubny, I., 1999. Fractional-order systems and PID controllers. IEEE Trans. Autom. Control 44 (1), 208–214.
Ramezanian, H., Balochian, S., Zare, A., 2013. Design of optimal fractional-order PID controllers using particle swarm optimization algorithm for automatic voltage regulator (AVR) system. J. Control Autom. Electr. Syst. 24 (5), 601–611.
Sahu, B.K., Pati, S., Mohanty, P.K., Panda, S., 2015. Teaching-learning based optimization algorithm based fuzzy-pid controller for automatic generation control of multi-area power system. Appl. Soft Comput. 27, 240–249.
Sakthivel, R., Shi, P., Arunkumar, A., Mathiyalagan, K., 2016. Robust reliable h∞ control for fuzzy systems with random delays and linear fractional uncertainties. Fuzzy Sets Syst. 302, 65–81.
Sharma, R., Gaur, P., Mittal, A., 2016. Design of two-layered fractional order fuzzy logic controllers applied to robotic manipulator with variable payload. Appl. Soft Comput. 47, 565–576.
Sharma, R., Rana, K., Kumar, V., 2014. Performance analysis of fractional order fuzzy pid controllers applied to a robotic manipulator. Expert. Syst. Appl. 41 (9), 4274–4289.
Shi, P., Su, X., Li, F., 2016. Dissipativity-based filtering for fuzzy switched systems with stochastic perturbation. IEEE Trans. Autom. Control 61 (6), 1694–1699.
Sun, B., Gui, W., Wang, Y., Yang, C., 2014. Intelligent optimal setting control of a cobalt removal process. J. Process Control 24 (5), 586–599.
Takahashi, M., 2016. Self-repairing pi/pid control against sensor failures. Int. J. Innov. Comput. Inf. Control. 12 (1), 193–202.
Wang, G., Yang, C., Zhu, H., Li, Y., Peng, X., Gui, W., 2016. State-transition-algorithm-based resolution for overlapping linear sweep voltammetric peaks with high signal ratio. Chemom. Intell. Lab. Syst. 151, 61–70.
Xie, Y., Xie, S., Chen, X., Gui, W., Yang, C., Caccetta, L., 2015. An integrated predictive model with an on-line updating strategy for iron precipitation in zinc hydro-metallurgy. Hydrometallurgy 151, 62–72.
Xie, Y., Xie, S., Li, Y., Yang, C., Gui, W., 2017. Dynamic modeling and optimal control of goethite process based on the rate-controlling step. Control. Eng. Pract. 58, 54–65.

Zamani, M., Karimi-Ghartemani, M., Sadati, N., Parniani, M., 2009. Design of a fractional order pid controller for an avr using particle swarm optimization. Control. Eng. Pract. 17 (12), 1380–1387.
Zhang, B., Yang, C., Gui, W., 2016a. Control strategy for hydrometallurgical removal process based on modelling and evaluation. IFAC-PapersOnLine 49 (20), 161–166.
Zhang, B., Yang, C., Zhu, H., Li, Y., Gui, W., 2013. Kinetic modeling and parameter estimation for competing reactions in copper removal process from zinc sulfate solution. Ind. Eng. Chem. Res. 52 (48), 17074–17086.
Zhang, B., Yang, C., Zhu, H., Li, Y., Gui, W., 2016b. Evaluation strategy for the control of the copper removal process based on oxidation-reduction potential. Chem. Eng. J. 284, 294–304.
Zhang, F., Yang, C., Zhou, X., Gui, W., 2016c. Fractional-order pid controller tuning using continuous state transition algorithm. Neural Comput. & Applic. 1–10. http://dx.doi.org/10.1007/s00521-016-2605-0.
Zhao, J., Bose, B.K., 2002. Evaluation of membership functions for fuzzy logic controlled induction motor drive. In: IEEE 28th Annual Conference of the Industrial Electronics Society. 1. pp. 229–234.
Zhou, X., Gao, D.Y., Yang, C., Gui, W., 2016. Discrete state transition algorithm for unconstrained integer optimization problems. Neurocomputing 173, 864–874.
Zhou, X., Shi, P., Lim, C.C., Yang, C., Gui, W., 2018. A dynamic state transition algorithm with application to sensor network localization. Neurocomputing 273, 237–250.
Zhou, X., Yang, C., Gui, W., 2012. State transition algorithm. J. Ind. Manag. Optim. 8 (4), 1039–1056.